CrystEngComm

PAPER

View Article Online
View Journal | View Issue

Cite this: *CrystEngComm*, 2024, **26**, 1962

Introduction of new guest molecules into BEDT-TTF radical-cation salts with tris(oxalato)ferrate†

Toby J. Blundell, [ab] Elizabeth K. Rusbridge,[a] Rebecca E. Pemberton,[a] Michael J. Brannan,[a] Alexander L. Morritt, [a] Joseph O. Ogar, [a] John D. Wallis, [a] Hiroki Akutsu, [c] Yasuhiro Nakazawa,[c] Shusaku Imajo[d] and Lee Martin *[a]

Received 1st February 2024,
Accepted 1st March 2024

DOI: 10.1039/d4ce00099d

rsc.li/crystengcomm

Radical-cation salts of formula β″-(BEDT-TTF)$_4$[(H$_3$O)Fe(C$_2$O$_4$)$_3$]·guest have produced a large number of superconductors and provided a route to introduce magnetism and chirality into the same multifunctional material. A relationship has been found in these salts between the length of the *b* axis and the superconducting Tc. Increasing the *b* axis length by introducing larger guest molecules, such as benzonitrile and nitrobenzene, gives the highest superconducting Tcs in this family of salts. Smaller guests such as pyridine show no superconducting transition, whilst asymmetrical guests which are larger than nitrobenzene have given a different bilayered structure. Other potential guest molecules have been limited by their ability to be used as the solvent in which the crystals are grown *via* electrocrystallisation. This paper reports a method which introduces guest molecules into the crystal which are a solid or liquid additive within the crystal-growing solvent 1,2,4-trichlorobenzene:ethanol. We present the crystal structures of five new BEDT-TTF radical-cation salts with tris(oxalato)ferrate anions using guest molecules toluene, phenol, benzaldehyde, 4-bromobenzaldehyde, and kojic acid.

Introduction

The donor molecule BEDT-TTF has produced the largest number of organic superconductors, with κ-(BEDT-TTF)$_2$Cu[N(CN)$_2$]Br (ref. 1) having the highest superconducting Tc at ambient pressure of 11.6 K, and β′-(BEDT-TTF)$_2$ICl$_2$ the highest Tc under pressure, 14.2 K.[2] These radical-cation salts are constructed of alternating conducting donor layers and insulating anion layers. Multifunctionality can be achieved through the introduction of anions or guest molecules into the insulating layer which combines their properties with the (super)conductivity of the BEDT-TTF layers.[3] The extensive family of BEDT-TTF radical-cation salts with the tris(oxalato) metallate anion combine conductivity with magnetism,[4] proton conductivity,[5] or chirality[6] in the same material.

The highest superconducting Tc in these salts is 8.5 K in β″-(BEDT-TTF)$_4$[(H$_3$O)Fe(C$_2$O$_4$)$_3$]·benzonitrile, which was also the first in this family to be discovered in 1995.[7] A polymorph of this salt which differs only in the spatial arrangement of the Δ and Λ Fe(C$_2$O$_4$)$_3^{3-}$ enantiomers and the disordered benzonitrile guest molecule is a semiconductor with pseudo-κ BEDT-TTF packing.[8] This shows the sensitivity of the conducting properties to changes in the BEDT-TTF salts due to subtle changes in the packing of the adjacent anion layers. The anion layers are a honeycomb arrangement of Fe(C$_2$O$_4$)$_3^{3-}$ and counter cation of H$_3$O$^+$, K$^+$, or NH$_4^+$ with a guest molecule of the solvent that is used for crystal growth situated within the hexagonal cavities in the honeycomb.[9]

Taking β″-(BEDT-TTF)$_4$[(H$_3$O)Fe(C$_2$O$_4$)$_3$]·benzonitrile as the starting point and changing the counter cation (H$_3$O$^+$, K$^+$, NH$_4^+$)[8,9] or changing the metal centre of the Fe(C$_2$O$_4$)$_3^{3-}$ anion has only small effect upon the donor packing and the conductivity. Changing the metal ion to Al^{3+},[10] Co^{3+},[10] Cr^{3+},[11] Ga^{3+},[12] Mn^{3+},[13] Rh^{3+},[14] or Ru^{3+},[10,15] does however change the magnetic moments in the anion layer. A much more pronounced effect upon the conducting properties results from changing the guest molecule within the anion layer hexagonal cavity.

[a] *School of Science and Technology, Nottingham Trent University, Clifton Lane, Clifton, Nottingham, NG11 8NS, UK. E-mail: lee.martin@ntu.ac.uk*
[b] *Department of Chemistry, University of Durham, Stockton Road, Durham, DH1 3LE, UK*
[c] *Department of Chemistry, Graduate School of Science, Osaka University, 1-1 Machikaneyama-cho, Toyonaka, Osaka 560-0043, Japan*
[d] *The Institute for Solid State Physics, The University of Tokyo, Kashiwa, Chiba 277-8581, Japan*

† Electronic supplementary information (ESI) available: CCDC 2324160–2324164 contains supplementary X-ray crystallographic data for (**I**)–(**V**), respectively. For crystallographic data in CIF or other electronic format see DOI: https://doi.org/10.1039/d4ce00099d

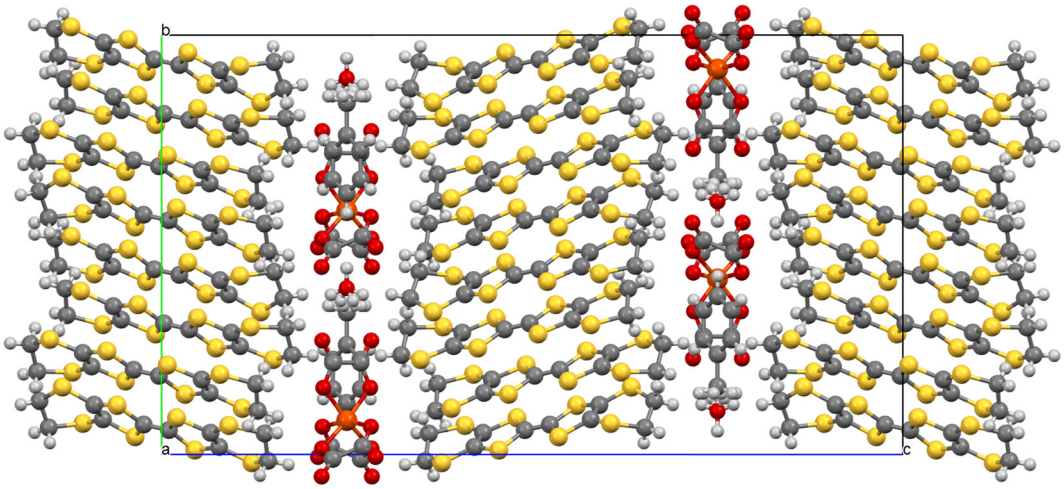

Fig. 1 β″-(BEDT-TTF)$_4$[(H$_3$O)Fe(C$_2$O$_4$)$_3$]·toluene (I) viewed down the *a* axis.

The shape, the size, and the orientation of the guest molecule within the anion layer all influence the packing and the disorder of the ethylene groups of adjacent donors which has a marked effect on the conducting behaviour and can destabilise the superconducting transition.[16]

Using guest molecules close in size to benzonitrile gives isostructural β″-(BEDT-TTF)$_4$[(H$_3$O)Fe(C$_2$O$_4$)$_3$]·guest salts whose cell parameters can be correlated with the conducting properties.[17] The superconducting Tc is shown to increase with increasing length of the *b* axis.[17] The –C≡N bond of the benzonitrile molecule is directed along the *b* axis, so increased length of the guest molecule can increase the Tc. A good example of this is in the halobenzene series where higher Tcs are observed for the larger bromobenzene and iodobenzene salts, whilst the fluorobenzene and chlorobenzene salts remain metallic down to 0.8 K.[12,14,18]

A different structure is obtained when using much smaller guests such as nitromethane or acetonitrile where a 3:1 semiconducting phase is obtained.[19] When using larger guests such as *sec*-phenethyl alcohol, acetophenone, or 1,2-dibromobenzene, the molecule protrudes from the anion layer on one side. This gives each anion layer two different faces which leads to a different donor packing on each side of the anion layer *e.g.* α,β″ or α,pseudo-κ.[20] It is also possible for the 18-crown-6, used to aid tris(oxalato)metallate solubility, to be included in the hexagonal cavity. This has produced both a 2:1 proton conductor[6] and 2:1 superconductors.[21,22]

Although the origin of the superconductivity in the β″-(BEDT-TTF)$_4$[(H$_3$O)Fe(C$_2$O$_4$)$_3$]·guest family is of interest in terms of its unconventional mechanism,[23] the search for higher Tcs in the β″-(BEDT-TTF)$_4$[(H$_3$O)Fe(C$_2$O$_4$)$_3$]·guest family has been limited by the ability of the guest molecule solvent to grow crystals. This paper reports the introduction of new guest molecules into the crystal which are a solid or liquid additive within the crystal-growing solvent 1,2,4-trichlorobenzene:ethanol which provides a route to introducing a variety of new guests into salts of this type. We present the crystal structures of five new BEDT-TTF radical-cation salts with tris(oxalato)ferrate anions using guest

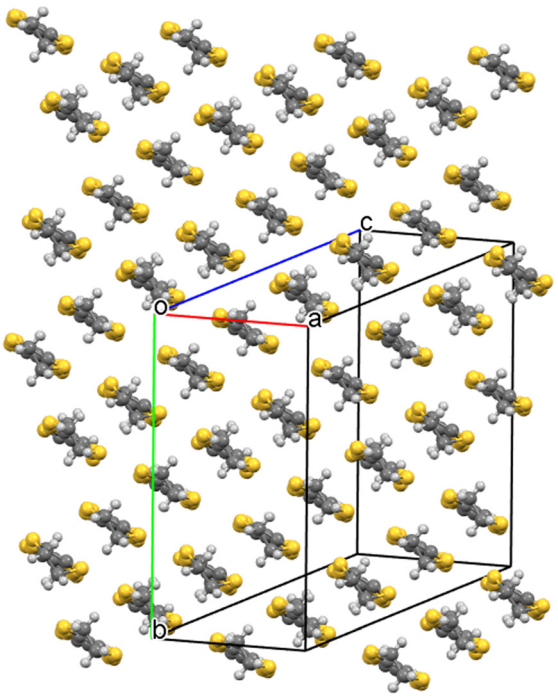

Fig. 2 β″-(BEDT-TTF)$_4$[(H$_3$O)Fe(C$_2$O$_4$)$_3$]·toluene (I) donor layer.

Table 1 Short S···S contacts (<sum VdW radii) in β″-(BEDT-TTF)$_4$[(H$_3$O)Fe(C$_2$O$_4$)$_3$]·toluene (I)

S atom 1	S atom 2	Contact/Å
S1	S7	3.404(3)
S2	S9	3.299(3)
S2	S11	3.350(3)
S3	S7	3.469(3)
S6	S15	3.475(3)
S8	S15	3.501(3)
S8	S10	3.566(3)

Table 2 Approximation of the charge of BEDT-TTF molecules in β″-(BEDT-TTF)$_4$[(H$_3$O)Fe(C$_2$O$_4$)$_3$]·toluene (I) from bond lengths (Å): $\delta = (b + c) - (a + d)$, $Q = 6.347–7.463\delta$ (ref. 24)

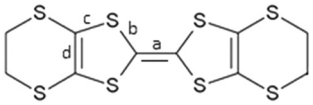

Donor	*a*	*b*	*c*	*d*	*δ*	*Q*
A	1.369	1.740	1.753	1.354	0.770	0.60+
B	1.361	1.741	1.753	1.352	0.781	0.52+

molecules toluene, phenol, benzaldehyde, kojic acid, and 4-bromobenzaldehyde.

Results and discussion

The aim was to introduce new guest molecules into the hexagonal cavity of superconducting salts of β″-(BEDT-TTF)$_4$[(A)M(C$_2$O$_4$)$_3$]·guest where currently benzonitrile and nitrobenzene give the highest Tcs.[9] The desired 4 : 1 β″-(BEDT-TTF)$_4$[(A)M(C$_2$O$_4$)$_3$]·guest formula has been obtained when using toluene, phenol or benzaldehyde as the guest molecule. Novel structures have been obtained including a 5 : 1 BEDT-TTF salt when using 4-bromobenzaldehyde as the guest molecule and a 4 : 1 BEDT-TTF salt when using kojic acid where kojate replaces one of the bidentate oxalate ligands of the anion.

β″-(BEDT-TTF)$_4$[(H$_3$O)Fe(C$_2$O$_4$)$_3$]·toluene (I)

β″-(BEDT-TTF)$_4$[(H$_3$O)Fe(C$_2$O$_4$)$_3$]·toluene crystallises in monoclinic space group *C*2/*c* and has an asymmetric unit of two crystallographically independent BEDT-TTF donor molecules, 0.5 of a tris(oxalato)ferrate anion, 0.5 of a toluene molecule and 0.5 of a H_3O^+ cation. The Fe atom, toluene and oxonium oxygen atom lie on two-fold axes. The donors and anions form segregated stacks (Fig. 1) with the BEDT-TTF donors having a β″ packing arrangement with the two crystallographically independent donors adopting an ···AABBAA··· packing order within a stack (Fig. 2). Table 1 shows the intermolecular S···S close contacts between donor molecules which are similar to other salts in this series of 4 : 1 salts, with a network of interactions between BEDT-TTF molecules in neighbouring stacks providing the conducting network. Table 2 shows the estimation of charge on the donor molecules based on the bond lengths which are close to the 0.5^+ expected for these salts.[9]

The anion layer (Fig. 3) is a hexagonal arrangement of tris(oxalato)metallate anions and H_3O cation with a toluene guest in the hexagonal cavity with the $-CH_3$ group directed along the *b* axis. Each anion layer consists of a single enantiomer of tris(oxalato)ferrate with the next anion layer consisting only of the opposite enantiomer, to give an overall racemic lattice.

The highest superconducting Tcs in this series of salts are found when the *b* axis length of the crystal structure is elongated by the inclusion of solvents such as benzonitrile and nitrobenzene.[9] The desired 4 : 1 β″-(BEDT-TTF)$_4$[(A)M(C$_2$O$_4$)$_3$]·guest has been obtained when using toluene as the guest molecule. However, the *b* axis length is shorter

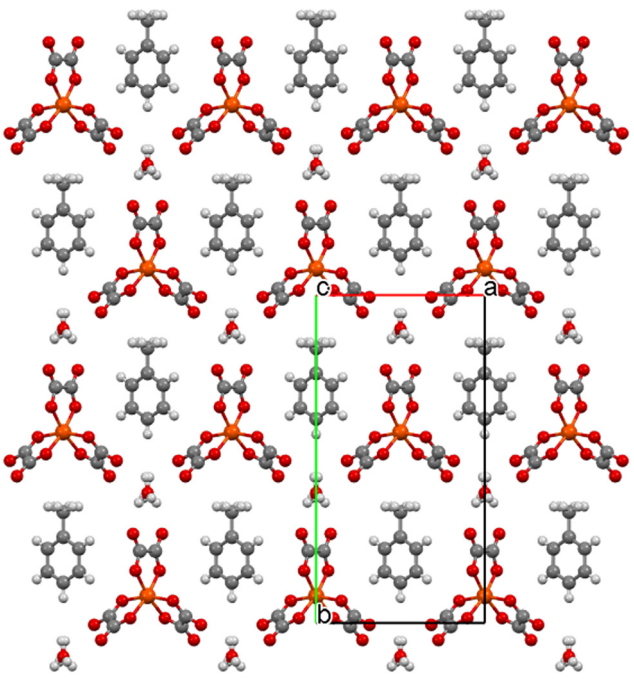

Fig. 3 β″-(BEDT-TTF)$_4$[(H$_3$O)Fe(C$_2$O$_4$)$_3$]·toluene (I) anion layer viewed down the *c* axis.

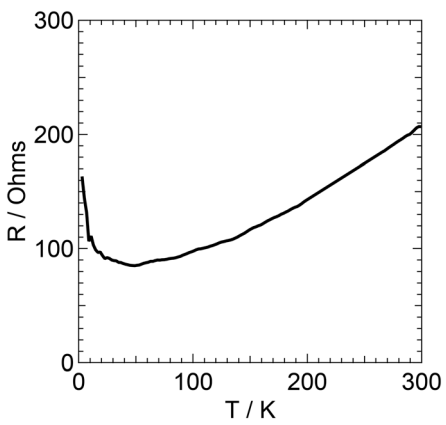

Fig. 4 β″-(BEDT-TTF)$_4$[(H$_3$O)Fe(C$_2$O$_4$)$_3$]·toluene (I) electrical resistance.

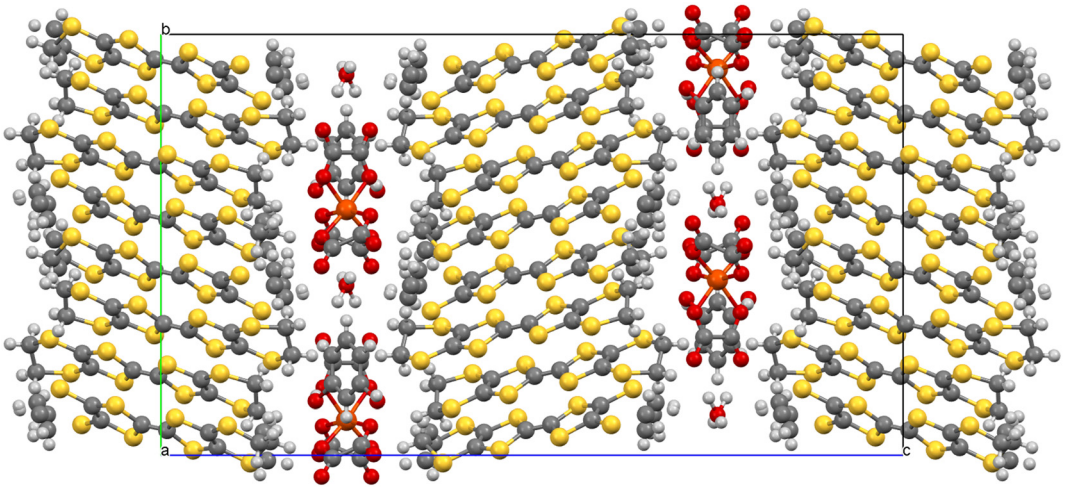

Fig. 5 β″-(BEDT-TTF)$_4$[(H$_3$O)Fe(C$_2$O$_4$)$_3$]·phenol (**II**) viewed down the *a* axis.

(19.9069(14) Å at 150 K in Fe/toluene) compared to the isostructural Fe/benzonitrile (20.04(3) Å at 120 K) and Fe/nitrobenzene (19.9494(3) Å at 120 K) salts which exhibit the highest superconducting Tcs in this family of salts.[9] The superconducting Tc would therefore be expected to be lower than the Fe/benzonitrile and Fe/nitrobenzene salts if superconductivity is present. The other superconducting salts with a monosubstituted-benzene guest and tris(oxalato) ferrate (Fe/bromobenzene, Fe/fluorobenzene, Fe/2-bromopyridine, and Fe/2-chloropyridine) undergo a transition to lower symmetry at around 200 K so their *b* axes are therefore not comparable with salt (**I**) at 120 K.[9] Salts Fe/3-chloropyridine and Fe/3-bromopyridine in space group *C*2/*c* remain metallic down to 0.4 K and do not undergo a superconducting transition, and they have shorter *b* axes of 19.8295(3) Å (at 120 K) and 19.8214(3) Å (at 100 K), respectively.[9]

Fig. 4 shows the electrical resistance measurements for β″-(BEDT-TTF)$_4$[(H$_3$O)Fe(C$_2$O$_4$)$_3$]·toluene which shows metallic behaviour from room temperature down to 50 K then an upturn in resistance below 50 K. In addition, SQUID magnetometry was performed on a polycrystalline sample down to 1.8 K and no Meissner signal was observed.

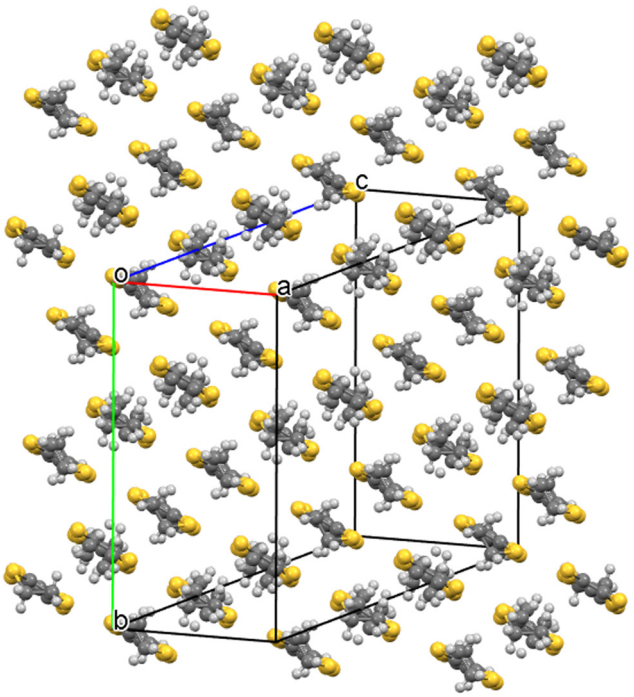

Fig. 6 β″-(BEDT-TTF)$_4$[(H$_3$O)Fe(C$_2$O$_4$)$_3$]·phenol (**II**) donor layer.

β″-(BEDT-TTF)$_4$[(H$_3$O)Fe(C$_2$O$_4$)$_3$]·phenol (II)

Salt (**II**) (Fig. 5) is isostructural with (**I**) with β″ donor packing (Fig. 6). Table 3 shows the S⋯S close contacts and Table 4 the estimation of charge on the donor molecules, which are again close to the expected 0.5$^+$.[9] The anion layer (Fig. 7) has the hexagonal arrangement of tris(oxalato)ferrate anions and H$_3$O cation with a phenol guest in the hexagonal cavity. It's usual in 4 : 1 β″-(BEDT-TTF)$_4$[(A)M(C$_2$O$_4$)$_3$]·guest for the R group of the monosubstituted benzene guest molecule to be directed along the *b* axis, but this is not the case for the –OH group of phenol where the –OH is disordered over two positions (Fig. 7).

The *b* axis length is shorter (20.0206(5) Å at 298 K in Fe/phenol) compared to the isostructural Fe/benzonitrile (20.1539(8) Å at 293 K) and Fe/nitrobenzene (20.0908(3) Å at 298 K) salts which exhibit the highest superconducting Tcs in

Table 3 Short S⋯S contacts (<sum VdW radii) in β″-(BEDT-TTF)$_4$[(H$_3$O)Fe(C$_2$O$_4$)$_3$]·phenol (**II**)

S atom 1	S atom 2	Contact/Å
S1	S7	3.5436(9)
S5	S7	3.4014(9)
S4	S15	3.5517(10)
S6	S9	3.3941(10)
S6	S13	3.3642(10)

Table 4 Approximation of the charge of BEDT-TTF molecules in β″-(BEDT-TTF)$_4$[(H$_3$O)Fe(C$_2$O$_4$)$_3$]·phenol (**II**) from bond lengths (Å): $\delta = (b + c) - (a + d)$, $Q = 6.347–7.463\delta$ (ref. 24)

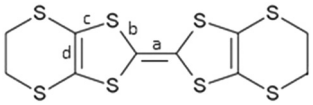

Donor	*a*	*b*	*c*	*d*	*δ*	*Q*
A	1.366	1.7423	1.7515	1.351	0.777	0.55+
B	1.368	1.73975	1.7505	1.3485	0.774	0.57+

this family of salts.[9] There are several other superconducting salts with a monosubstituted-benzene guest and tris(oxalato) ferrate that have a published room temperature crystal structure [Fe/bromobenzene T_c = 4 K (b = 20.0546(15) Å), Fe/fluorobenzene T_c = <1 K (b = 20.0280(10) Å), Fe/2-bromopyridine T_c = 4 K (b = 20.0265(5) Å), and Fe/2-chloropyridine T_c = 2.4–4.0 K (b = 19.9856(6) Å)].[9] Salts which remain metallic down to 0.4 K and do not show superconductivity having room temperature crystal structures are Fe/chlorobenzene (b = 20.0124(10) Å) and Fe/2-bromopyridine (b = 20.0265(5) Å). Fig. 8 shows the electrical resistance measurements for (**II**) with metallic behaviour from room temperature down to 10 K then an upturn in resistance down to 0.5 K, with no transition to the superconducting state down to 0.5 K.

β″–β″-(BEDT-TTF)$_4$[(H$_3$O)Fe(C$_2$O$_4$)$_3$]·benzaldehyde (III)

Salt (**III**) (Fig. 9) has β″ donor packing (Fig. 10) and the same 4 : 1 formula as salts (**I**) and (**II**). The anion layer (Fig. 11) has the expected honeycomb packing with the asymmetrical benzaldehyde guest molecule in the hexagonal cavity with the –CHO group directed along the b axis.

Table 5 shows the S···S close contacts and Table 6 shows the estimation of charge on the donor molecules, which are in some cases slightly higher than the expected 0.5$^+$.

Salts (**I**) and (**II**) crystallise in monoclinic space group $C2/c$, however at 150 K the crystal structure of (**III**) shows triclinic symmetry. This structural phase transition has been reported previously when the guest molecule is a 2-halopyridine, but not when it is a 3-halopyridine.[25] Calculation of a C-centred cell for salt (**III**) would give a b axis of 19.920 Å at 150 K which is longer than that the b axis of metallic salt (**I**) (19.9069(14) Å at 150 K in Fe/toluene) and closer to the superconducting Fe/nitrobenzene (19.9494(3) Å at 120 K).[9] Electrical resistance measurements for (**III**) (Fig. 12) show a metal–insulator transition at 190 K and SQUID magnetometry was performed on a polycrystalline sample down to 1.8 K with no Meissner signal observed. It has been concluded previously that ordering of a non-symmetrical guest, such as benzaldehyde, may prevent a superconducting transition owing to the dipole moment.[26]

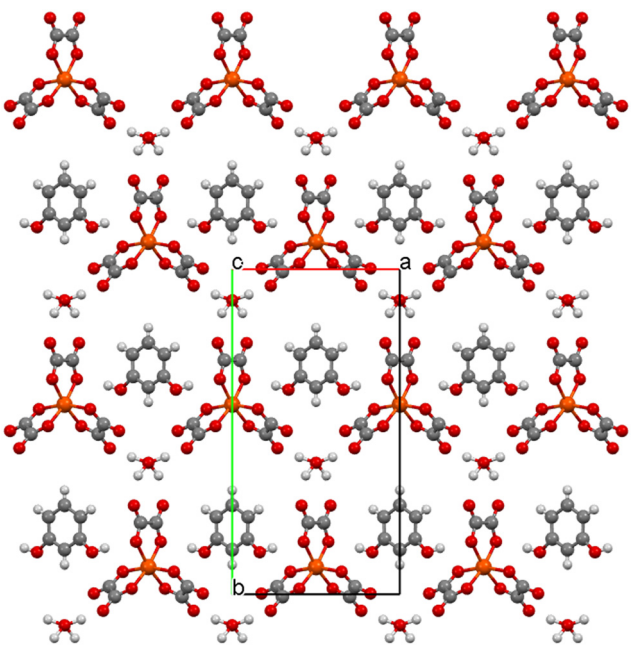

Fig. 7 β″-(BEDT-TTF)$_4$[(H$_3$O)Fe(C$_2$O$_4$)$_3$]·phenol (**II**) anion layer viewed down the c axis showing the 50 : 50 disorder of the –OH group of phenol over two positions.

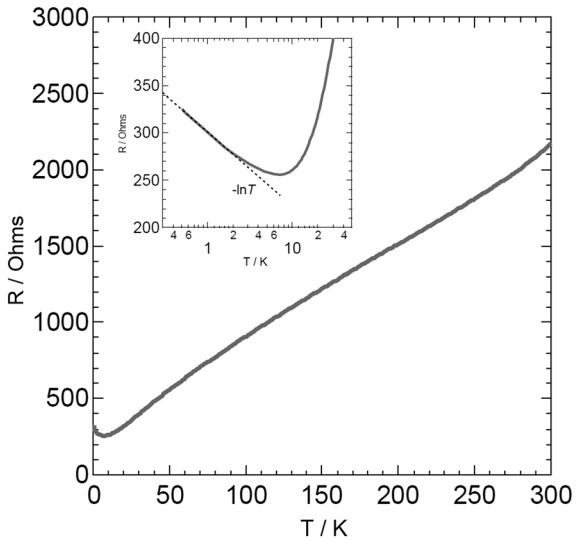

Fig. 8 β″-(BEDT-TTF)$_4$[(H$_3$O)Fe(C$_2$O$_4$)$_3$]·phenol (**II**) electrical resistance. The inset shows an upturn in the resistance below 10 K.

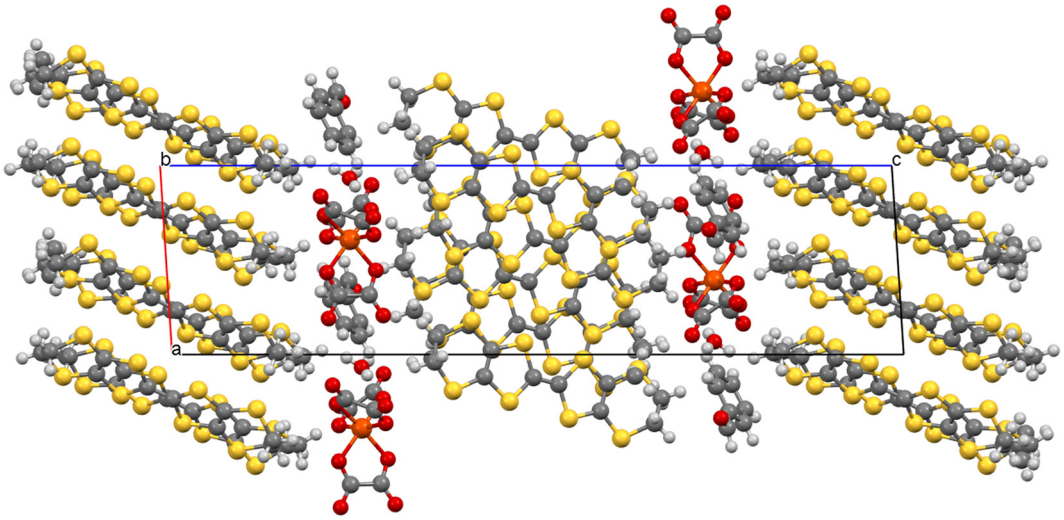

Fig. 9 β″–β″-(BEDT-TTF)$_4$[(H$_3$O)Fe(C$_2$O$_4$)$_3$]·benzaldehyde (**III**) viewed down the *b* axis.

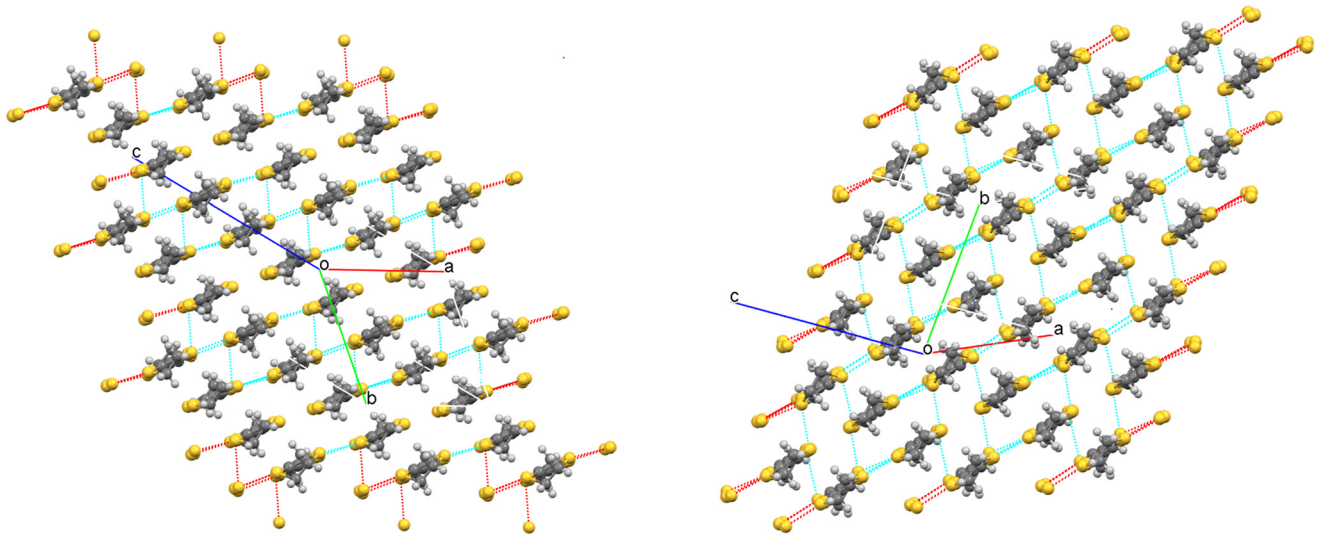

Fig. 10 β″–β″-(BEDT-TTF)$_4$[(H$_3$O)Fe(C$_2$O$_4$)$_3$]·benzaldehyde (**III**) donor layers showing close S···S contact. β″ layer at the centre of the unit cell *c* axis (left) and β″ layer at the end of the unit cell (right).

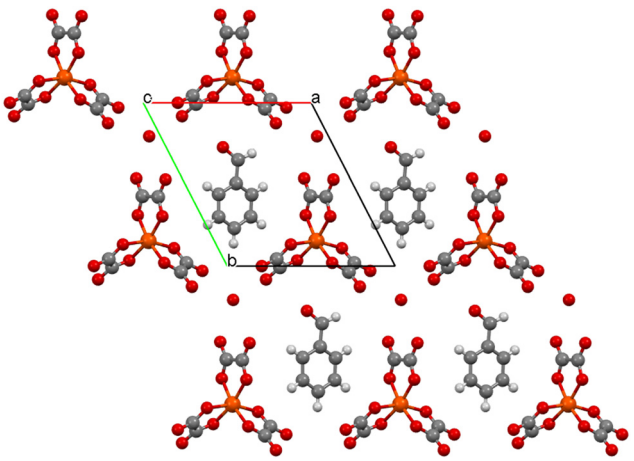

Fig. 11 β″–β″-(BEDT-TTF)$_4$[(H$_3$O)Fe(C$_2$O$_4$)$_3$]·benzaldehyde (**III**) anion layer viewed down the *c* axis.

β″-β‴-(BEDT-TTF)$_5$[Fe(C$_2$O$_4$)$_3$]·ethanol·2H$_2$O (IV)

Increasing the size of the guest molecule from benzaldehyde in (**III**) to 4-bromobenzaldehyde in (**IV**) gives a 5 : 1 salt instead of a 4 : 1 salt like (**I**)–(**III**). The 4-bromobenzaldehyde molecule is not included in the crystal. β″–β‴-(BEDT-TTF)$_5$[Fe(C$_2$O$_4$)$_3$]·ethanol·2H$_2$O (**IV**) crystallises in triclinic space group $P\bar{1}$ with an asymmetric unit of four crystallographically independent BEDT-TTF donor molecules plus two half BEDT-TTF molecules, one tris(oxalato)ferrate anion, one ethanol molecule and two H$_2$O molecules.

The donors and anions form segregated stacks (Fig. 13) with two crystallographically independent BEDT-TTF layers (Fig. 14). One BEDT-TTF layer has a β″ packing motif (Fig. 14 and 15 left) whilst we have given the other BEDT-TTF layer a prefix of β‴ (Fig. 14 and 15 right). This β‴ donor layer consists of stacks which are built up of trimers (cyan-white-cyan,

Table 5 Short S···S contacts (<sum VdW radii) in β″–β″-(BEDT-TTF)$_4$[(H$_3$O)Fe(C$_2$O$_4$)$_3$]·benzaldehyde (**III**)

S atom 1	S atom 2	Contact/Å
S2C	S8D	3.525(5)
S7C	S6D	3.447(6)
S7C	S8D	3.541(7)
S3C	S2D	3.377(6)
S1C	S2D	3.316(7)
S6C	S7D	3.595(4)
S3D	S7D	3.390(6)
S1D	S7D	3.380(6)
S3B	S7B	3.496(4)
S1B	S7B	3.394(5)
S6B	S2A	3.516(4)
S8B	S2A	3.547(6)
S2B	S6A	3.343(4)
S2B	S8A	3.314(6)
S1B	S2A	3.582(5)

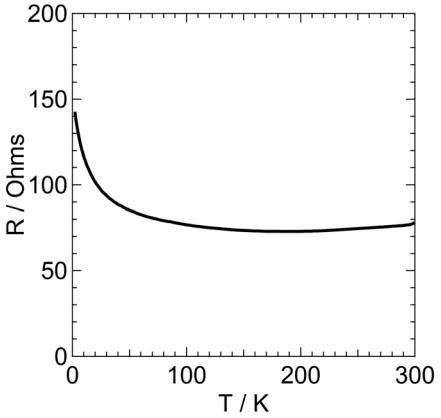

Fig. 12 β″–β″-(BEDT-TTF)$_4$[(H$_3$O)Fe(C$_2$O$_4$)$_3$]·benzaldehyde (**III**) electrical resistance.

Fig. 15) in a β″-type ring-over-atom arrangement, alternating with dimers (purple, Fig. 15) which are in a β ring-over-bond arrangement.[27] The dimer (purple) is tilted by 8.3° compared to the trimer (cyan-white-cyan) within a donor stack (Fig. 16 right). By contrast the other crystallographically independent layer in this structure has no tilt between the trimer (red-yellow-red) and dimer (blue) and is purely β″-type ring-over-atom (Fig. 16 left). This difference can be attributed to the position of the dimers in relation to the tris(oxalato) ferrate enantiomers in the neighbouring anion layers. Each anion layer consists of a single enantiomer so the two faces of an anion layer are different due to the propeller twist of the three oxalate ligands around the Fe centre. Fig. 16 shows the locations of the tris(oxalato)ferrate anions at each face of the donor layer relative to the dimers of the two crystallographically independent donor stacks. The inner oxygen of the oxalate ligand nearest to the donor stack is much closer for the purple donor (C27···O10 3.180(7) Å) compared to the blue donor (C10···O9 3.598(7) Å).

The tris(oxalato)ferrates are arranged in a parallellogram with an ethanol and two water molecules (Fig. 17). Each anion layer consists of a single enantiomer of tris(oxalato) ferrate with the next anion layer consisting only of the opposite enantiomer, to give an overall racemic lattice.

This salt is isostructural with a previously reported structure where the included guest molecule is dichloromethane rather than ethanol, β″-(BEDT-TTF)$_5$[Fe(C$_2$O$_4$)$_3$]·dichloromethane·2H$_2$O.[28]

Table 7 shows the S···S close contacts and Table 8 shows the estimation of charge on the donor molecules. The anion layer has a charge of 3− to be balanced by five BEDT-TTF molecule, which would approximate to 0.6+ each. The estimated donor charges (Table 8, Fig. 15) are larger than expected at 0.69–0.88^{+}.

Raman and XPS spectra for the previously published isostructural dichloromethane salt[27] show peaks corresponding to both BEDT-TTF$^{0.5+}$ and BEDT-TTF^{1+}. The dichloromethane salt showed semiconducting behaviour but crystals of (**IV**) were unsuitable for electrical resistivity measurement. Reliable electrical resistivity data could not be obtained on (**IV**) due to surface degradation and decomposed impurities deposited on the surface of the crystals. Even if the crystals were formed into pellets, it would be difficult to accurately measure electrical resistance due to the high contact resistance at the grain boundary between the crystals.

α‴″-(BEDT-TTF)$_4$[Fe(oxalate)$_2$(kojate)] (**V**)

The use of kojic acid (Scheme 1) as the guest has produced a new salt of formula α‴″-(BEDT-TTF)$_4$[Fe(oxalate)$_2$(kojate)] (**V**).

Table 6 Approximation of the charge of BEDT-TTF molecules in β″–β″-(BEDT-TTF)$_4$[(H$_3$O)Fe(C$_2$O$_4$)$_3$]·benzaldehyde (**III**) from bond lengths (Å): $\delta = (b + c) - (a + d)$, $Q = 6.347–7.463\delta$ (ref. 24)

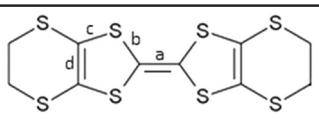

Donor	*a*	*b*	*c*	*d*	*δ*	*Q*
A	1.357	1.7425	1.751	1.350	0.787	0.48+
B	1.372	1.7345	1.7565	1.349	0.770	0.60+
C	1.355	1.7393	1.7443	1.3465	0.782	0.51+
D	1.376	1.734	1.751	1.355	0.754	0.72+

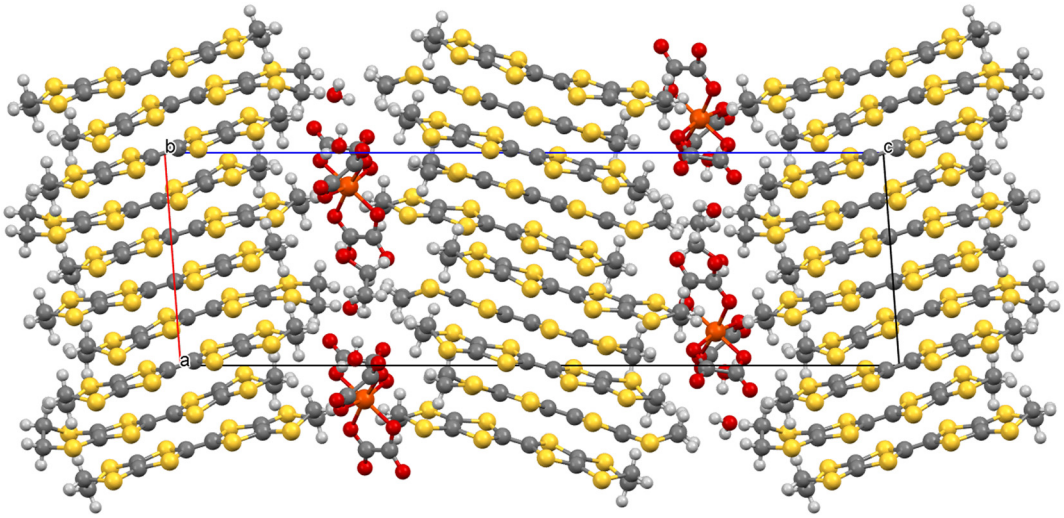

Fig. 13 β″–β‴-(BEDT-TTF)$_5$[Fe(C$_2$O$_4$)$_3$]·ethanol·2H$_2$O (**IV**) viewed down the *b* axis.

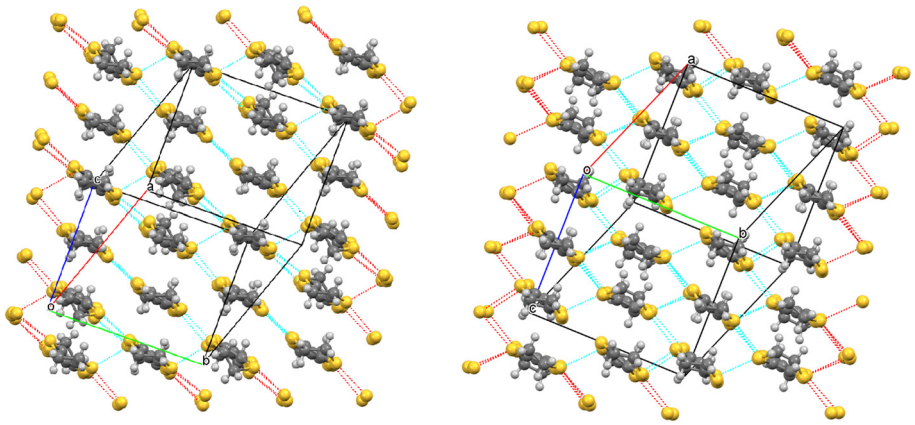

Fig. 14 Donor packing in β″–β‴-(BEDT-TTF)$_5$[Fe(C$_2$O$_4$)$_3$]·ethanol·2H$_2$O (**IV**) showing close S···S contact. β″ layer on the end of the unit cell *c* axis (left) and β‴ layer at the centre of the unit cell (right).

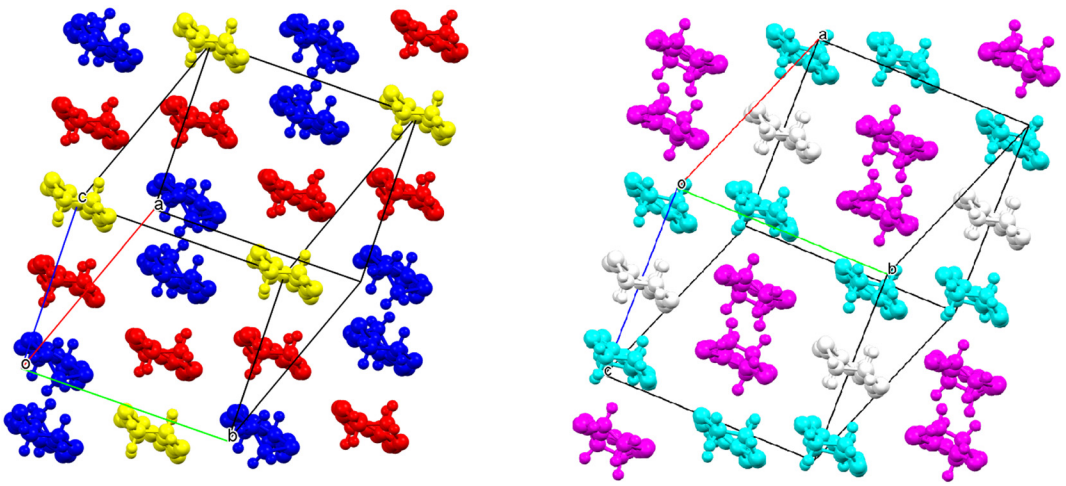

Fig. 15 Donor packing in β″–β‴-(BEDT-TTF)$_5$[Fe(C$_2$O$_4$)$_3$]·ethanol·2H$_2$O (**IV**) showing colours for the crystallographically independent donors. β″ layer on the end of the unit cell *c* axis (left) and β‴ layer at the centre of the unit cell (right).

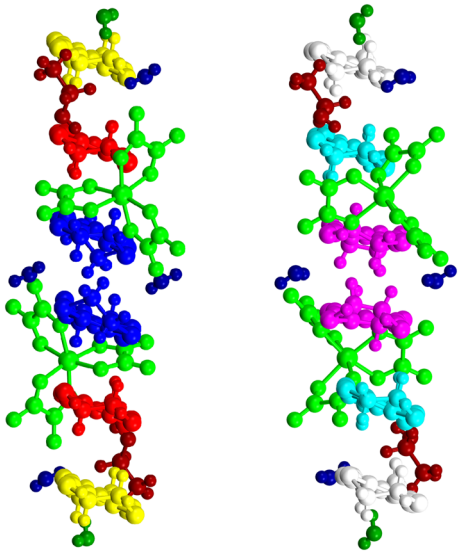

Fig. 16 Donor packing within a stack in β″–β‴-(BEDT-TTF)$_5$[Fe(C$_2$O$_4$)$_3$]·ethanol·2H$_2$O (**IV**) showing colours for the crystallographically independent donors and the position of the neighbouring tris(oxalato)ferrate anions above and below the dimer sites. β‴ layer on the end of the unit cell *c* axis (left) and β″ layer at the centre of the unit cell (right).

Salt (**V**) crystallises in space group *P*2/*n* and has an asymmetric unit of eight crystallographically independent BEDT-TTF donor molecules and two Fe(oxalate)$_2$(kojate) anions. Under the conditions of electrocrystallisation one of the bidentate oxalate ligands on tris(oxalato)ferrate has been replaced with a kojic acid.

The donors and anions form segregated stacks (Fig. 18) with the BEDT-TTF donors having a packing not previously observed which, following convention, has been called α‴ packing (Fig. 19). Neighbouring donor stacks B, C, and D (Fig. 19) pack in the manner of β″-type packing, whilst neighbouring stacks D, A, B pack in an α-type packing.

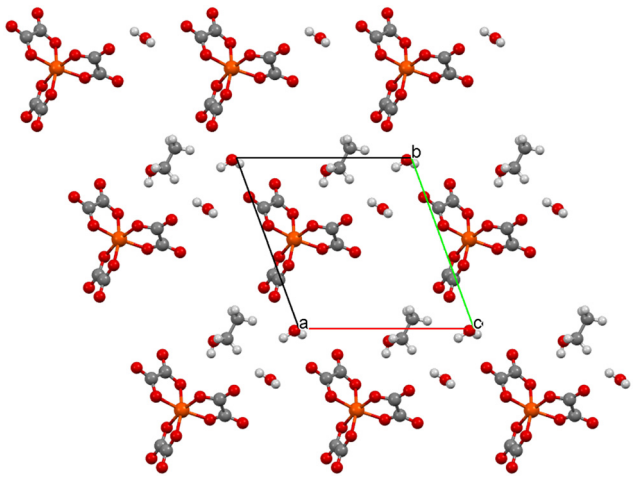

Fig. 17 Anion layer in β″–β‴-(BEDT-TTF)$_5$[Fe(C$_2$O$_4$)$_3$]·ethanol·2H$_2$O (**IV**) viewed down the *c* axis.

Table 7 Short S···S contacts (<sum VdW radii) in β″–β‴-(BEDT-TTF)$_5$[Fe(C$_2$O$_4$)$_3$]·ethanol·2H$_2$O (**IV**)

S atom 1	S atom 2	Contact/ Å
S2	S16	3.450(2)
S8	S10	3.545(2)
S8	S20	3.553(2)
S1	S18	3.360(2)
S3	S18	3.473(2)
S7	S17	3.495(2)
S7	S19	3.532(2)
S9	S15	3.362(2)
S11	S15	3.470(2)
S22	S34	3.587(2)
S26	S30	3.534(2)
S21	S33	3.471(3)
S22	S37	3.382(2)
S22	S39	3.447(2)
S21	S38	3.430(2)
S21	S40	3.536(2)
S25	S37	3.429(2)
S27	S37	3.504(2)
S30	S34	3.504(2)

Table 9 shows the S···S close contacts which are all side-to-side between adjacent stacks with no face-to-face S···S contacts. Table 10 shows the estimation of charge on the eight crystallographically independent BEDT-TTF donor molecules (Fig. 20). The overall charge for the eight BEDT-TTF is estimated as 5.4+. The Fe(oxalate)$_2$(kojate) anion has a charge of 2− so an average charge of 0.5+ per BEDT-TTF, and an overall for the eight BEDT-TTFs of 4+, is expected. There is charge localisation in this structure at room temperature with the donor stack which is tilted at an angle to the others (claret and light blue donors in Fig. 20) having BEDT-TTF$^{0.32+}$ and BEDT-TTF$^{0.49+}$ whilst BEDT-TTFs in the other layers have higher charges of between 0.67+ and 0.85+ (Table 10).

The anion layer (Fig. 21) consists of only Fe(oxalate)$_2$(kojate) anions which alternate in each stack between the Δ and the Λ enantiomers to give a racemic structure.

Electrical resistivity has been measured on single crystals of this salt which shows metallic behaviour from room temperature down to 100 K, below which there is transition to the insulating state (Fig. 22). SQUID magnetometry was performed on a polycrystalline sample down to 1.8 K but no Meissner signal was observed.

Conclusions

We present five new radical-cation salts of BEDT-TTF with tris(oxalato)ferrate anions. Three are 4 : 1 salts β″-(BEDT-TTF)$_4$[(H$_3$O)Fe(C$_2$O$_4$)$_3$]·guest (guest = toluene, phenol, benzaldehyde) which are metallic at room temperature but none show a superconducting transition at lower temperatures. The *b* axes in these salts are shorter than those where the guest is nitrobenzene or benzonitrile, which have the highest superconducting Tc in this family of salts. A 5 : 1 salt of formula β″–β‴-(BEDT-TTF)$_5$[Fe(C$_2$O$_4$)$_3$]·ethanol·2H$_2$O

Table 8 Approximation of the charge of BEDT-TTF molecules in β″–β‴-(BEDT-TTF)$_5$[Fe(C$_2$O$_4$)$_3$]·ethanol·2H$_2$O (**IV**) from bond lengths (Å): $\delta = (b + c) - (a + d)$, $Q = 6.347–7.463\delta$ (ref. 24)

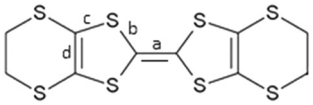

Donor	*a*	*b*	*c*	*d*	*δ*	*Q*
DARK BLUE	1.373	1.731	1.7415	1.3525	0.747	0.77+
RED	1.368	1.734	1.7455	1.354	0.758	0.69+
YELLOW	1.367	1.727	1.744	1.364	0.740	0.82+
MAGENTA	1.375	1.727	1.7383	1.348	0.742	0.81+
CYAN	1.386	1.729	1.743	1.354	0.732	0.88+
WHITE	1.378	1.7325	1.7485	1.355	0.748	0.77+

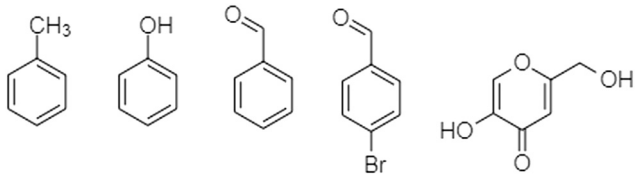

Scheme 1 From left to right, toluene, phenol, benzaldehyde, 4-bromobenzaldehyde, and kojic acid.

has a bilayered donor packing owing to the two different faces of the enantiomers of the tris(oxalato)ferrate anion being presented to each crystallographically independent donor layer. A new anion has been synthesised where a bidentate oxalate ligand of a tris(oxalato)ferrate has been replaced by kojic acid to give Fe(oxalate)$_2$(kojate) which has produced a 4 : 1 radical-cation salt with BEDT-TTF adopting a novel alpha‴ packing motif. The synthetic method offers the potential of allowing a multitude of solid guest molecules to be introduced into these salts where this was previously limited only to solvents used for growing the crystals. This method creates the possibility of introducing a guest which will extend the *b* axis and increase the superconducting Tc in this family of salts, and also of introducing a guest into the cavity which adds further functionality to the material.

Experimental

Starting materials

Ammonium tris(oxalato)ferrate, 1,2,4-trichlorobenzene, ethanol, phenol, toluene, benzaldehyde, kojic acid, 4-bromobenzaldehyde, and 18-crown-6 were purchased from Sigma-Aldrich and used as received. BEDT-TTF was purchased from TCI and recrystallised from chloroform.

Synthesis of radical-cation salts

Salt (**I**) was synthesised by adding 100 mg of ammonium tris(oxalato)ferrate, 300 mg 18-crown-6, and 10 ml of toluene to 10 ml 1,2,4-trichlorobenzene:2 ml ethanol and stirring

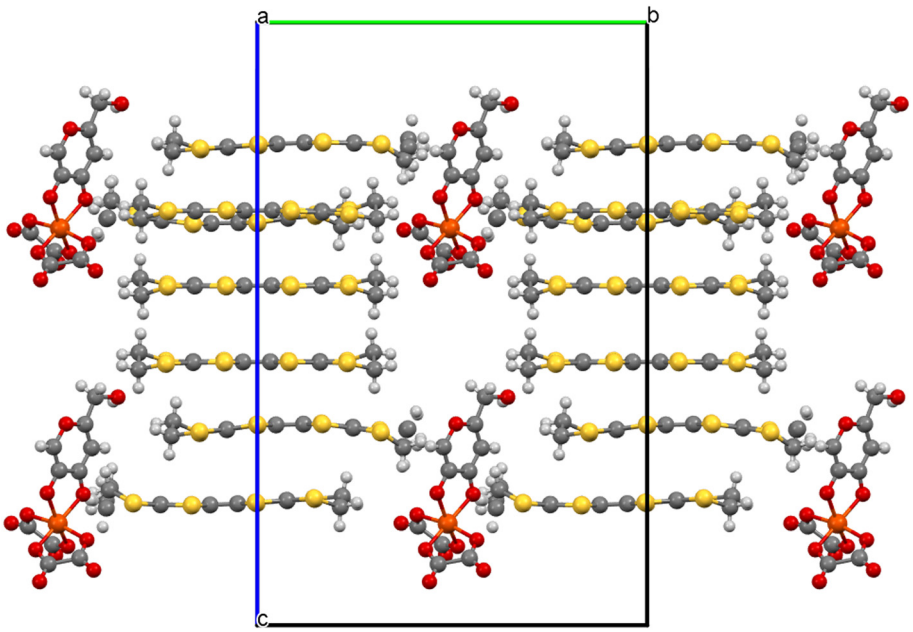

Fig. 18 α‴-(BEDT-TTF)$_4$[Fe(oxalate)$_2$(kojate)] (**V**) viewed down the *a* axis.

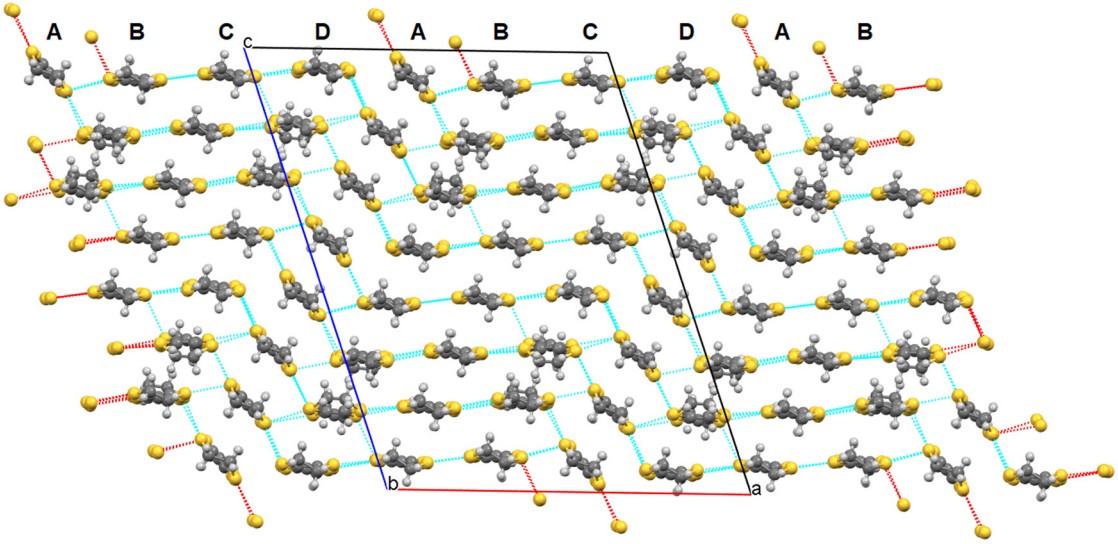

Fig. 19 α‴′-(BEDT-TTF)$_4$[Fe(oxalate)$_2$(kojate)] (**V**) donor layer showing close S···S contacts.

overnight before filtering into a H-cell containing 10.5 mg BEDT-TTF in the anode side. A current of 1.0 μA was applied for 1 week, then increased to 2.0 μA to give black blocks which were collected after 2 weeks.

Table 9 Short S···S contacts (<sum VdW radii) in α‴′-(BEDT-TTF)$_4$[Fe(oxalate)$_2$(kojate)] (**V**)

S atom 1	S atom 2	Contact/Å
S7E	S8F	3.583(3)
S4E	S2D	3.506(3)
S2E	S2D	3.386(3)
S8E	S6D	3.549(3)
S8E	S8D	3.418(3)
S3E	S2G	3.455(3)
S1E	S2G	3.581(3)
S1C	S2F	3.467(3)
S1C	S4F	3.547(3)
S7C	S8F	3.426(3)
S5C	S7F	3.596(3)
S1C	S1F	3.583(2)
S6C	S7D	3.573(3)
S8C	S7D	3.394(3)
S2C	S1D	3.404(3)
S2C	S3D	3.482(3)
S6C	S7B	3.568(3)
S2B	S4H	3.552(3)
S6B	S8H	3.475(3)
S8B	S8H	3.434(3)
S2B	S2H	3.460(3)
S2G	S3H	3.582(3)
S8G	S7H	3.568(3)
S2G	SH1	3.575(3)
S7G	S3H	3.536(3)
S1G	S7H	3.537(3)
S6A	S7F	3.597(3)
S8A	S7F	3.479(3)
S2A	S3F	3.546(3)
S2A	S1F	3.558(3)
S1A	S1B	3.455(3)
S1A	S3B	3.491(3)
S5A	S7B	3.535(3)
S7A	S7B	3.399(3)

Salt (**II**) was synthesised by adding 100 mg of ammonium tris(oxalato)ferrate, 250 mg 18-crown-6, and 100 mg of phenol to 15 ml 1,2,4-trichlorobenzene:3 ml ethanol and stirring overnight before filtering into a H-cell containing 10 mg BEDT-TTF in the anode side. A current of 0.5 μA was applied for 3 weeks to give black blocks.

Salt (**III**) was synthesised by adding 100 mg of ammonium tris(oxalato)ferrate, 300 mg 18-crown-6, and 10 ml of benzaldehyde to 10 ml 1,2,4-trichlorobenzene:2 ml ethanol and stirring overnight before filtering into a H-cell containing 16.6 mg BEDT-TTF in the anode side. A current of 1.0 μA was applied for 1 week, then increased to 2.0 μA to give black blocks which were collected after 2 weeks.

Salt (**IV**) was synthesised by adding 1 g of 4-bromobenzaldehyde to 20 ml 1,2,4-trichlorobenzene:2.5 ml ethanol and stirring overnight before filtering to remove any undissolved 4-bromobenzaldehyde. 100 mg of ammonium tris(oxalato)ferrate and 200 mg 18-crown-6 and a further 20 ml of 1,2,4-trichlorobenzene was then added to this solution with further stirring for 2 days. This was then filtered into a H-cell containing 10.5 mg BEDT-TTF in the anode side and a current of 1.0 μA was applied for 4 weeks to give black blocks.

Salt (**V**) was synthesised by adding 100 mg of ammonium tris(oxalato)ferrate, 250 mg 18-crown-6, and 100 mg of kojic acid to 15 ml 1,2,4-trichlorobenzene:3 ml ethanol and stirring overnight before filtering into a H-cell containing 10.5 mg BEDT-TTF in the anode side. A current of 0.5 μA was applied for 18 days to give black blocks.

Electrical resistivity measurements

Electrical resistance measurements were performed using physical properties measurement system (PPMS). Using attached four contacts on single crystals of (**I**), (**II**), (**III**) and (**V**), a current of 10 μA was applied in the conduction plane,

Table 10 Approximation of the charge of BEDT-TTF molecules in α‴-(BEDT-TTF)$_4$[Fe(oxalate)$_2$(kojate)] (**V**) from bond lengths (Å): $\delta = (b + c) - (a + d)$, $Q = 6.347–7.463\delta$ (ref. 24)

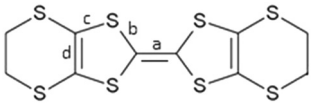

Donor	*a*	*b*	*c*	*d*	*δ*	*Q*
WHITE	1.385	1.73075	1.74625	1.351	0.741	0.82+
GREEN	1.374	1.73475	1.74275	1.3515	0.752	0.74+
MAGENTA	1.386	1.7295	1.74525	1.3515	0.737	0.85+
RED	1.375	1.7335	1.7435	1.360	0.742	0.81+
YELLOW	1.378	1.73525	1.7505	1.3515	0.756	0.70+
DARK BLUE	1.366	1.738	1.746	1.3575	0.761	0.67+
CLARET	1.356	1.74125	1.75725	1.335	0.808	0.32+
CYAN	1.352	1.73775	1.7505	1.351	0.785	0.49+

and in-plane resistance was measured. The samples were cooled down to 2 K at a cooling rate of 1 K min^{-1}. Data for samples (**I**), (**II**) and (**III**) are presented with the unit of Ohms, rather than resistivity because the long axis of the crystals was one approximately 0.2–0.3 mm. Consequently, accurately estimating the crystal thickness and the distance between terminals was challenging, making it difficult to convert the obtained resistance into resistivity. Crystals of and (**IV**) were unsuitable for measurement. Reliable electrical resistivity data could not be obtained on (**IV**) due to surface degradation and decomposed impurities deposited on the surface of the crystals. Even if the crystals were formed into pellets, it would be difficult to accurately measure electrical resistance due to the high contact resistance at the grain boundary between the crystals.

X-ray crystallography

Data were collected on a Rigaku Oxford Diffraction Xcalibur System equipped with a Sapphire detector using MoKα radiation at 150 K for (**I**), (**III**) and at 293 K for (**IV**).

Data were collected on ere collected on a Rigaku *R*-AXIS VII imaging plate system with FR-E SuperBright High-Brilliance Rotating Anode Generator with confocal monochromated MoKα radiation, using a Rapid Auto software for control and processing, at 298 K for (**II**) and 293 K for (**V**).

Crystal data for (**I**): at 150 K: $C_{53}H_{44}FeO_{13}S_{32}$, M = 1970.65, black needle, a = 10.2478(6), b = 19.9069(14), c = 35.264(2) Å, β = 94.106(5)°, U = 7175.5(8) Å^3, T = 150.00(10) K, space group $C2/c$, Z = 4, μ = 10.914 mm^{-1}, reflections collected = 14 834, independent reflections = 6875, R_1 = 0.0865, wR_2 = 0.2084 [$F^2 > 2\sigma(F^2)$], R_1 = 0.1221, wR_2 = 0.2440 (all data). CCDC 2324160.

Crystal data for (**II**): at 298 K: $C_{52}H_{39}FeO_{14}S_{32}$, M = 1970.65, black needle, a = 10.3279(3), b = 20.0206(5), c = 35.3409(9) Å, β = 92.910(7)°, U = 7298.0(4) Å^3, T = 298.0 K, space group $C2/c$, Z = 4, μ = 11.828 mm^{-1}, reflections collected = 34 328, independent reflections = 8371, R_1 = 0.0382, wR_2 = 0.0849 [$F^2 > 2\sigma(F^2)$], R_1 = 0.0540, wR_2 = 0.0919 (all data). CCDC 2324162.

Crystal data for (**III**): at 150 K: $C_{53}H_{41}FeO_{14}S_{32}$, M = 1983.63, black block, a = 10.2331(10), b = 11.1922(9), c = 35.2191(14) Å, α = 89.485(5), β = 86.524(6), γ = 62.861(9)°, U =

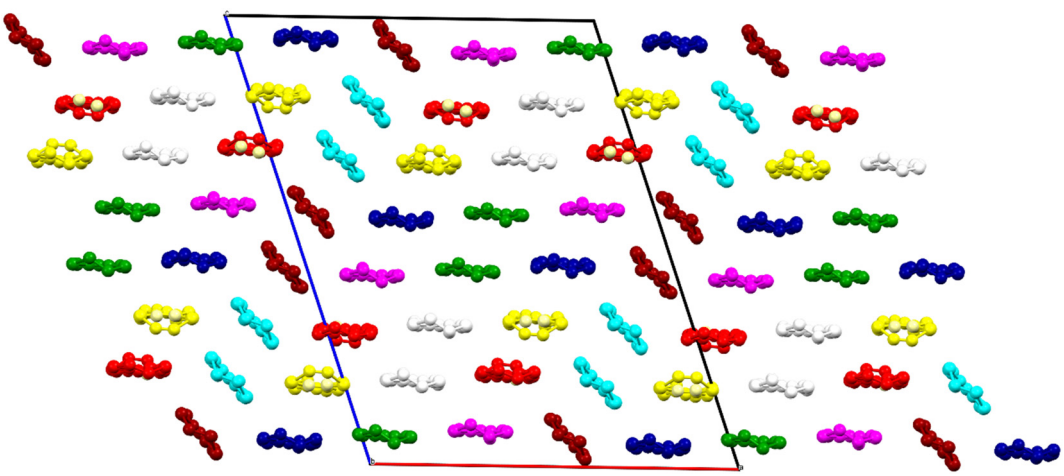

Fig. 20 α‴-(BEDT-TTF)$_4$[Fe(oxalate)$_2$(kojate)] (**V**) donor layer showing colours for the crystallographically independent donors.

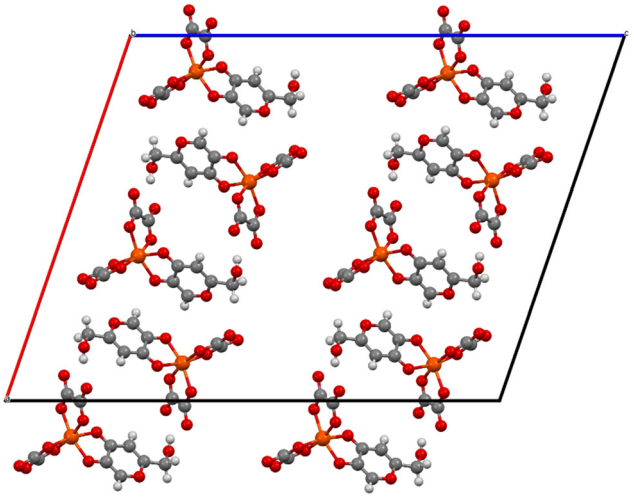

Fig. 21 α‴′-(BEDT-TTF)$_4$[Fe(oxalate)$_2$(kojate)] (**V**) anion layer viewed down the c axis.

3582.2(5) Å^3, T = 150.00(10) K, space group $P\bar{1}$, Z = 2, μ = 10.948 mm^{-1}, reflections collected = 13 676, independent reflections = 9317, R_1 = 0.1380, wR_2 = 0.3903 [$F^2 > 2\sigma(F^2)$], R_1 = 0.1767, wR_2 = 0.4400 (all data). CCDC 2324161.

Crystal data for (**IV**): at 293 K: $C_{56}H_{44}FeO_{14}S_{40}$, M = 2279.20, black plate, a = 11.1233(2), b = 11.5487(2), c = 35.1801(6) Å, α = 89.381(6), β = 85.771(6), γ = 69.934(5)°, U = 4232.87(19) Å^3, T = 293 K, space group $P\bar{1}$, Z = 2, μ = 1.223 mm^{-1}, reflections collected = 44 010, independent reflections = 14 933, R_1 = 0.0595, wR_2 = 0.0844 [$F^2 > 2\sigma(F^2)$], R_1 = 0.1699, wR_2 = 0.1863 (all data). CCDC 2324163.

Crystal data for (**V**): at 293 K: $C_{50}H_{37}FeO_{12}S_{32}$, M = 1911.56, black prism, a = 24.9368(6), b = 19.4833(3), c = 31.827(10) Å, β = 108.849(3)°, U = 14634.6(7) Å^3, T = 293(2) K, space group $P2/n$, Z = 8, μ = 10.671 mm^{-1}, reflections collected = 100 711, independent reflections = 28 105, R_1 = 0.0707, wR_2 = 0.1793 [$F^2 > 2\sigma(F^2)$], R_1 = 0.1528, wR_2 = 0.2308 (all data). CCDC 2324164.

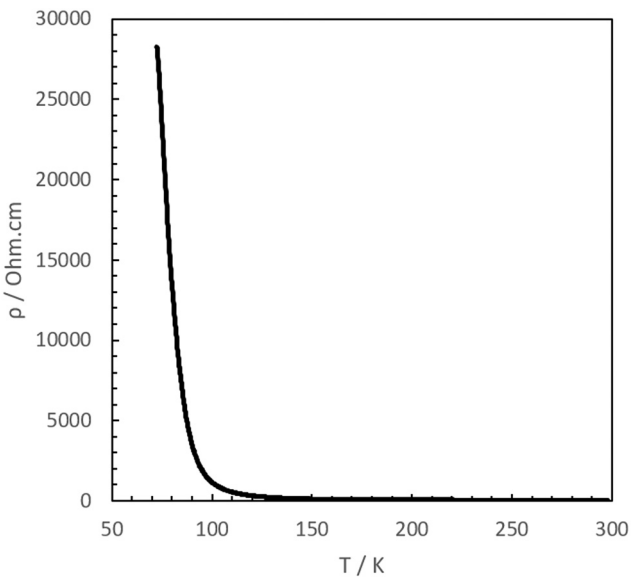

Fig. 22 α‴′-(BEDT-TTF)$_4$[Fe(oxalate)$_2$(kojate)] (**V**) electrical resistivity.

Author contributions

Synthesis, RP, MB, ALM, EKR, LM; X-ray crystallography, TJB, JOO, LM; conductivity measurements SI, EKR, HA, YN; writing-original draft preparation, LM; project administration, LM; funding acquisition, LM; supervision, LM, JDW, TJB, JOO.

Conflicts of interest

There are no conflicts to declare.

Acknowledgements

LM, JO and TJB would like to thank the Leverhulme Trust for financial support (RPG-2019-242). EKR would like to thank NTU for a PhD studentship. EKR, LM, HA, and YN would like to thank JSPS for funding the Summer Program for EKR.

References

1 A. M. Kini, U. Geiser, H. H. Wang, K. D. Carlson, J. M. Williams, W. K. Kwok, K. G. Vandervoort, J. E. Thompson and D. L. Stupka, *Inorg. Chem.*, 1990, **29**, 2555–2557.
2 H. Taniguchi, M. Miyashita, K. Uchiyama, K. Satoh, N. Mori, H. Okamoto, K. Miyagawa, K. Kanoda, M. Hedo and Y. Uwatoko, *J. Phys. Soc. Jpn.*, 2003, **72**, 468–471.
3 P. Day and E. Coronado, *Chem. Rev.*, 2004, **11**, 5419–5448.
4 B. Zhang, Y. Zhang and D. Zhu, *Chem. Commun.*, 2012, **48**, 197–199; E. Coronado, J. R. Galán-Mascarós, C. J. Gómez-García and V. Laukhin, *Nature*, 2000, **408**, 447–449; A. Alberola, E. Coronado, J. R. Galán-Mascarós, C. Giménez-Saiz and C. J. Gómez-García, *J. Am. Chem. Soc.*, 2003, **125**, 10774–10775.
5 A. Akutsu-Sato, H. Akutsu, S. S. Turner, P. Day, M. R. Probert, J. A. K. Howard, T. Akutagawa, S. Takeda, T. Nakamura and T. Mori, *Angew. Chem., Int. Ed.*, 2005, **44**, 291–295.
6 L. Martin, P. Day, H. Akutsu, J-i. Yamada, S-i. Nakatsuji, W. Clegg, R. W. Harrington, P. N. Horton, M. B. Hursthouse, P. McMillan and S. Firth, *CrystEngComm*, 2007, **10**, 865–867.
7 A. W. Graham, M. Kurmoo and P. Day, *J. Chem. Soc., Chem. Commun.*, 1995, 2061–2062; M. Kurmoo, A. W. Graham, P. Day, S. J. Coles, M. B. Hursthouse, J. L. Caulfield, J. Singleton, F. L. Pratt and W. Hayes, *J. Am. Chem. Soc.*, 1995, **117**, 12209–12217.
8 L. Martin, S. S. Turner, P. Day, K. M. A. Malik, S. J. Coles and M. B. Hursthouse, *Chem. Commun.*, 1999, 513–514.
9 S. Benmansour and C. J. Gómez-García, *Magnetochemistry*, 2021, **7**, 93; L. Martin, *Coord. Chem. Rev.*, 2018, **376**, 277–291.
10 T. J. Blundell, M. Brannan, J. Mburu-Newman, H. Akutsu, Y. Nakazawa, S. Imajo and L. Martin, *Magnetochemistry*, 2021, **7**, 90.
11 L. Martin, S. S. Turner, P. Day, F. E. Mabbs and E. J. L. McInnes, *Chem. Commun.*, 1997, 1367–1368.

12 T. J. Blundell, A. L. Morritt, E. K. Rusbridge, L. Quibell, J. Oakes, H. Akutsu, Y. Nakazawa, S. Imajo, T. Kadoya, J.-i. Yamada, S. J. Coles, J. Christensen and L. Martin, *Mater. Adv.*, 2022, **3**, 4724–4735.
13 S. Benmansour, Y. Sánchez-Máñez and C. J. Gómez-García, *Magnetochemistry*, 2017, **3**, 7.
14 L. Martin, A. L. Morritt, J. R. Lopez, Y. Nakazawa, H. Akutsu, S. Imajo, Y. Ihara, B. Zhang, Y. Zhang and Y. Guo, *Dalton Trans.*, 2017, **46**, 9542–9548.
15 T. G. Prokhorova, L. V. Zorina, S. V. Simonov, V. N. Zverev, E. Canadell, R. P. Shibaeva and E. B. Yagubskii, *CrystEngComm*, 2013, **15**, 7048.
16 Y. Ihara and S. Imajo, *Crystals*, 2022, **12**(5), 711.
17 S. Imajo, H. Akutsu, A. Akutsu-Sato, A. L. Morritt, L. Martin and Y. Nakazawa, *Phys. Rev. Res.*, 2019, **1**, 033184.
18 E. Coronado, S. Curreli, C. Giménez-Saiz and C. J. Gómez-García, *Inorg. Chem.*, 2012, **51**, 1111–1126.
19 L. Martin, H. Akutsu, P. N. Horton and M. B. Hursthouse, *CrystEngComm*, 2015, **17**, 2783–2790; L. Martin, S.-i. Nakatsuji, J.-i. Yamada, H. Akutsu and P. Day, *J. Mater. Chem.*, 2010, **20**, 2738–2742; L. Martin, P. Day, S.-i. Nakatsuji, J.-i. Yamada, H. Akutsu and P. Horton, *CrystEngComm*, 2010, **12**, 1369–1372.
20 H. Akutsu, A. Akutsu-Sato, S. S. Turner, P. Day, E. Canadell, S. Firth, R. J. H. Clark, J. Yamada and S. Nakatsuji, *Chem. Commun.*, 2004, 18–19; L. V. Zorina, S. S. Khasanov, S. V. Simonov, R. P. Shibaeva, V. N. Zverev, E. Canadell, T. G. Prokhorova and E. B. Yagubskii, *CrystEngComm*, 2011, **13**, 2430–2438.
21 L. Martin, A. L. Morritt, J. R. Lopez, H. Akutsu, Y. Nakazawa, S. Imajo and Y. Ihara, *Inorg. Chem.*, 2017, **56**(2), 717–720.
22 L. Martin, J. R. Lopez, H. Akutsu, Y. Nakazawa and S. Imajo, *Inorg. Chem.*, 2017, **56**(22), 14045–14052; A. L. Morritt, J. R. Lopez, T. J. Blundell, E. Canadell, H. Akutsu, Y. Nakazawa, S. Imajo and L. Martin, *Inorg. Chem.*, 2019, **58**, 10656–10664.
23 S. Imajo, H. Akutsu, R. Kurihara, T. Yajima, Y. Kohama, M. Tokunaga, K. Kindo and Y. Nakazawa, *Phys. Rev. Lett.*, 2020, **125**, 177002.
24 P. Guionneau, C. J. Kepert, G. Bravic, D. Chasseau, M. R. Truter, M. Kurmoo and P. Day, *Synth. Met.*, 1997, **86**, 1973–1974.
25 T. G. Prokhorova, L. I. Buravov, E. B. Yagubskii, L. V. Zorina, S. V. Simonov, V. N. Zverev, R. P. Shibaeva and E. Canadell, *Eur. J. Inorg. Chem.*, 2015, 5611–5620.
26 T. G. Prokhorova, E. B. Yagubskii, A. A. Bardin, V. N. Zverev, G. V. Shilov and L. I. Buravov, *Magnetochemistry*, 2021, **7**, 83.
27 T. Mori, *Bull. Chem. Soc. Jpn.*, 1998, **71**, 2509.
28 B. Zhang, Y. Zhang, F. Liu and Y. Guo, *CrystEngComm*, 2009, **11**, 2523–2528.